

Spin transfer and critical current for magnetization reversal in ferromagnet-ferromagnet-ferromagnet double-barrier tunnel junctions

Xi Chen, Qing-Rong Zheng, and Gang Su*

*College of Physical Sciences, Graduate University of Chinese Academy of Sciences,
P.O. Box 4588, Beijing 100049, People's Republic of China*

(Received 2 May 2008; revised manuscript received 6 August 2008; published 16 September 2008)

In terms of the Keldysh nonequilibrium Green's-function method and invoking the generalized Landau-Lifshitz-Gilbert equation in presence of the spin-transfer torque (STT), we have systematically investigated the spin-transfer effect as well as the critical current for magnetization reversal in the ferromagnet (FM)-ferromagnet-ferromagnet double-barrier magnetic tunnel junctions. It has been found that the tunnel magnetoresistance (TMR) increases dramatically with the increase in the molecular field of the middle FM, and the larger the molecular field, the greater the TMR. The STT is found to oscillate with the bias voltage for finite thickness of the middle FM, while the electrical current as a function of the bias is almost linear with slight oscillations. It has been shown that the molecular field and the polarization dependences of the critical voltage and critical electrical current show steplike behaviors for finite thicknesses of the middle FM. The order of magnitude of the critical current is estimated to be about 10^5 – 10^6 A/cm². The present results are expected to be instructive for manufacturing the relevant spintronic devices.

DOI: [10.1103/PhysRevB.78.104410](https://doi.org/10.1103/PhysRevB.78.104410)

PACS number(s): 73.40.Gk, 75.60.Jk, 75.70.Cn

I. INTRODUCTION

In 1988, two different groups, independently, discovered an unusual large magnetoresistance in magnetic multilayers.^{1,2} This surprising discovery was then named as giant magnetoresistance (GMR) and thought to be a totally new phenomenon that is caused by spin-dependent scatterings of conduction electrons. Since then, a great number of research works focus on various circumstances of GMR effect in different systems, substantiating it to be a source of new scientific and technological applications. On the other hand, the development of GMR effect triggers the rediscovery of tunneling magnetoresistance (TMR) in magnetic tunnel junctions (MTJs). A single-barrier MTJ consists of two metallic ferromagnet (FM) electrodes separated by an insulating barrier. In 1975, Jullière³ first studied the magnetoresistance in the Fe-Ge-Co MTJ and found that the TMR ratio can be as high as 14%. A breakthrough has been made in 1995 that a large TMR has been reproducibly observed at room temperature in CoFe/Al₂O₃/Co (NiFe) and Fe/Al₂O₃/Fe MTJs.⁴ Recently, the use of a single-crystal MgO barrier in a MTJ has already generated a rather high TMR ratio, reaching 500%.⁵ In addition, the current-perpendicular-to-plane geometry of the MTJ makes it easy to be integrated into a nanoelectronic device, and in fact, the TMR-based read heads have been commercialized.⁶ These advances enable the TMR effect to possess even more essential industrial applications than the GMR effect in information storage and spin-based electronic devices. A significant progress has been made both experimentally and theoretically in the last decade.^{7–15}

An opposite phenomenon of GMR and TMR effects, coined as the spin-transfer effect (STE), was predicted independently by Berger¹⁶ and Slonczewski¹⁷ in 1996. STE states that when the spin-polarized electrons flowing from one FM layer into another FM layer with the magnetization aligned by a relative angle may transfer the transverse angular momenta to the local spins of the second FM layer, thereby

exerting a torque on the magnetic moments. By means of the STE, it is possible to switch the magnetic state of the free FM layer of a MTJ or spin valve by applying an electrical current instead of a magnetic field. This proposal was soon confirmed experimentally (e.g., Ref. 18). It is now well established that the STE could be applied to develop writing heads for magnetic random access memory (MRAM) or hard disk drivers. A nonvolatile STE memory has been demonstrated recently.¹⁹ In view of potentially wide use of the STE, a plenty of investigations concerning spin-transfer torque (STT) have been presented for different systems (e.g., Refs. 20–32).

On the other hand, the double-barrier magnetic tunnel junction (DBMTJ), in which the formation of quantum well states and the resonant tunneling phenomenon are anticipated, has attracted much attention in recent years. In order to observe the coherent tunneling through the DBMTJ, people have attempted to improve the junction quality to eliminate the influences from the interface roughness and impurity scattering, and remarkable advances have been achieved on this aspect (e.g., Refs. 33–36). One of the interesting DBMTJs is the FM-FM-FM DBMTJ, which is comprised of three metallic FM layers separated by double insulating barriers. It has been shown that the FM-FM-FM DBMTJs can be used as the basic elements for MRAM or DBMTJ-based spin transistors and have successfully been fabricated recently, where some peculiar properties have been observed.^{33,35} On account of the importance of such a nanostructure, it would be interesting to explore systematically the STE as well as the critical current for magnetization reversal in the presence of the STT in FM-FM-FM DBMTJs, as they are directly related to the practical realizations in possible spintronic devices.

The other parts of this paper are arranged as follows. In Sec. II, a model is proposed, and the relevant Green's functions are obtained in terms of the nonequilibrium Green's-function (NEGF) method. In Sec. III, the properties of STT in the system under consideration are numerically investi-

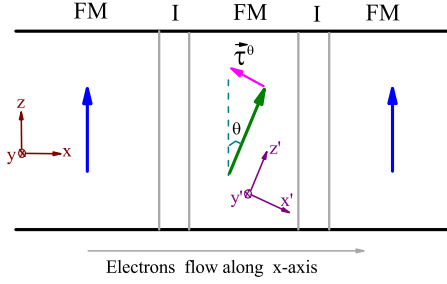


FIG. 1. (Color online) A schematic illustration of spin-transfer torque in a FM-I-FM-I-FM tunnel junction. Note that the electrons flow along the x axis.

gated, and some discussions are presented. The critical current for magnetization reversal of the middle FM layer in presence of the STT will be explored in Sec. IV. Finally, a brief summary will be given in Sec. V.

II. MODEL AND GREEN'S FUNCTIONS

The system under interest, as illustrated in Fig. 1, is composed of three metallic FMs separated by two thin insulators. The left (L) and right (R) ferromagnets, whose molecular fields are assumed to align along the z axis, are stretched to infinite, and the middle FM, whose orientation of magnetization is along the z' axis, deviating an angle θ from the z axis, is supposed to be several nanometers thick. The Hamiltonian of the system reads

$$H = H_L + H_R + H_C + H_{LC} + H_{CR}, \quad (1)$$

with

$$H_\alpha = \sum_{k_\alpha \sigma} \varepsilon_{k_\alpha \sigma} a_{k_\alpha \sigma}^\dagger a_{k_\alpha \sigma} \quad (\alpha = L, R), \quad (2)$$

$$\begin{aligned} H_C &= \sum_{k\sigma} \varepsilon_k c_{k\sigma}^\dagger c_{k\sigma} - \sum_k (c_{k\uparrow}^\dagger, c_{k\downarrow}^\dagger) \hat{\sigma} \cdot \vec{M} \begin{pmatrix} c_{k\uparrow} \\ c_{k\downarrow} \end{pmatrix} \\ &= \sum_{k\sigma} [(\varepsilon_k - \sigma M \cos \theta) c_{k\sigma}^\dagger c_{k\sigma} - M \sin \theta c_{k\sigma}^\dagger c_{k\bar{\sigma}}], \quad (3) \end{aligned}$$

$$H_{LC} = \sum_{k_L k \sigma \sigma'} (T_{k_L k}^{\sigma \sigma'} a_{k_L \sigma}^\dagger c_{k \sigma'} + \text{H.c.}), \quad (4)$$

$$H_{CR} = \sum_{k_R k \sigma \sigma'} (T_{k_R k}^{\sigma \sigma'} a_{k_R \sigma}^\dagger c_{k \sigma'} + \text{H.c.}), \quad (5)$$

where $a_{k_\alpha \sigma}$ and $c_{k\sigma}$ are annihilation operators of electrons with momentum k and spin σ in the α electrode and in the middle FM layer, respectively, $\varepsilon_{k_\alpha \sigma} = \varepsilon_{k_\alpha} - \sigma M_\alpha - eV_\alpha$ is the single-electron energy for the wave vector k_α with the molecular field M_α in the α electrode, ε_k is the single-electron energy, M is the molecular field that is proportional to the exchange constant in the middle FM layer, $\bar{\sigma} = -\sigma$, and $T_{k_\alpha k}^{\sigma \sigma'}$ are the tunneling matrix elements of electrons between the α electrode with spin σ and the middle FM layer with spin σ' .

In this paper, we assume that the middle FM is made of a soft magnetic material so that the magnetization is easier to

reverse and can be regarded as the free layer, while the side FMs can be treated as pinned layers. The spins in the middle FM can be written as^{11,20}

$$S^\theta = \frac{\hbar}{2} \sum_{k\mu\nu} c_{k\mu}^\dagger c_{k\nu} (R^{-1} \chi_\mu)^\dagger \hat{\sigma} (R^{-1} \chi_\nu), \quad (6)$$

where

$$R = \begin{pmatrix} \cos \frac{\theta}{2} & -\sin \frac{\theta}{2} \\ \sin \frac{\theta}{2} & \cos \frac{\theta}{2} \end{pmatrix},$$

$\hat{\sigma}$ is the Pauli matrix, and $\chi_{\mu(\nu)}$ denotes spin states. Note that Eq. (6) is written in the xyz coordinate frame, while the spins S^θ are quantized in the $x'y'z'$ coordinate frame. We can further write $S^\theta = \frac{\hbar}{2} \sum_k (\cos \theta c_{k\sigma}^\dagger c_{k\bar{\sigma}} - \sigma \sin \theta c_{k\sigma}^\dagger c_{k\sigma})$. Therefore, the spin torque, namely, the time evolution rate of the total spin of the middle FM, can be obtained by $\partial S^\theta / \partial t = \frac{i}{\hbar} \langle [H, S^\theta] \rangle$. According to Refs. 20, 37, and 38, the middle FM gains two types of torques: one is the equilibrium torque caused by the spin-dependent potential and the other is from the tunneling of electrons that is just what we are interested in. After cautiously separating the current-induced torques from the equilibrium one, the STT can be obtained,

$$\begin{aligned} \tau^\theta &= \frac{i}{\hbar} \langle [H_T, S^\theta] \rangle = \Re e \left[\sum_{k_L k} \text{Tr}_\sigma (\hat{\sigma}_1 \cos \theta \right. \\ &\quad \left. - \hat{\sigma}_3 \sin \theta) \hat{T}_{k_L k} \hat{G}_{kk_L}^<(t, t) \right], \quad (7) \end{aligned}$$

where

$$\hat{\sigma}_1 = \begin{pmatrix} 0 & 1 \\ 1 & 0 \end{pmatrix}, \quad \hat{\sigma}_3 = \begin{pmatrix} 1 & 0 \\ 0 & -1 \end{pmatrix}$$

are Pauli matrices,

$$\hat{T}_{k_L k} = \begin{pmatrix} T_{k_L k}^{\uparrow\uparrow} & T_{k_L k}^{\uparrow\downarrow} \\ T_{k_L k}^{\downarrow\uparrow} & T_{k_L k}^{\downarrow\downarrow} \end{pmatrix},$$

with the entities $T_{k_L k}^{\sigma \sigma'}$ being the tunneling matrix elements,

$$\hat{G}_{kk_L}^< = \begin{pmatrix} G_{kk_L}^{<\uparrow\uparrow} & G_{kk_L}^{<\uparrow\downarrow} \\ G_{kk_L}^{<\downarrow\uparrow} & G_{kk_L}^{<\downarrow\downarrow} \end{pmatrix}$$

are the lesser Green's functions in spin space, with the entities defined as $G_{kk_\alpha}^{<\sigma \sigma'}(t, t') = i \langle a_{k_\alpha \sigma'}^\dagger(t') c_{k\sigma}(t) \rangle$, and Tr_σ stands for the trace of the matrix taking over the spin space.

From Eq. (7), one may see that the current-induced STT can be obtained as long as we get the lesser Green's functions $G_{kk_\alpha}^{<\sigma \sigma'}$. In the following, we will use Keldysh's NEGF technique to determine all lesser Green's functions.³⁹ They are closely related to the retarded Green's functions that are defined by

$$G_{k\sigma k_\alpha \sigma'}^r(t, t') = -i \theta(t - t') \langle \{ c_{k\sigma}(t), a_{k_\alpha \sigma'}^\dagger(t') \} \rangle,$$

$$G_{k\sigma k\sigma'}^r(t, t') = -i\theta(t-t')\langle\{c_{k\sigma}(t), c_{k\sigma'}^\dagger(t')\}\rangle.$$

By using the equation of motion, we have

$$(\varepsilon - \varepsilon_{k_\alpha\uparrow})G_{k\uparrow k_\alpha\uparrow}^r(\varepsilon) = \sum_{k'} T_{k_\alpha k'}^{*\uparrow\uparrow} G_{k\uparrow k'\uparrow}^r(\varepsilon) + \sum_{k'} T_{k_\alpha k'}^{*\uparrow\downarrow} G_{k\uparrow k'\downarrow}^r(\varepsilon), \quad (8)$$

$$(\varepsilon - \varepsilon_{k_\alpha\uparrow})G_{k\downarrow k_\alpha\uparrow}^r(\varepsilon) = \sum_{k'} T_{k_\alpha k'}^{*\uparrow\uparrow} G_{k\downarrow k'\uparrow}^r(\varepsilon) + \sum_{k'} T_{k_\alpha k'}^{*\uparrow\downarrow} G_{k\downarrow k'\downarrow}^r(\varepsilon), \quad (9)$$

$$(\varepsilon - \varepsilon_{k_\alpha\downarrow})G_{k\uparrow k_\alpha\downarrow}^r(\varepsilon) = \sum_{k'} T_{k_\alpha k'}^{*\downarrow\downarrow} G_{k\uparrow k'\downarrow}^r(\varepsilon) + \sum_{k'} T_{k_\alpha k'}^{*\downarrow\uparrow} G_{k\uparrow k'\uparrow}^r(\varepsilon), \quad (10)$$

$$(\varepsilon - \varepsilon_{k_\alpha\downarrow})G_{k\downarrow k_\alpha\downarrow}^r(\varepsilon) = \sum_{k'} T_{k_\alpha k'}^{*\downarrow\downarrow} G_{k\downarrow k'\downarrow}^r(\varepsilon) + \sum_{k'} T_{k_\alpha k'}^{*\downarrow\uparrow} G_{k\downarrow k'\uparrow}^r(\varepsilon). \quad (11)$$

Obviously, to obtain the solution of $G_{k\sigma k_\alpha\sigma'}^r$, we have to get $G_{k\sigma k'\sigma'}^r$. For this purpose, we may apply the same procedure as that of obtaining Eqs. (8)–(11) and have

$$(\varepsilon - \varepsilon_{k'\uparrow} + M \cos \theta)G_{k\uparrow k'\uparrow}^r(\varepsilon) = -M \sin \theta G_{k\uparrow k'\downarrow}^r(\varepsilon) + \sum_{\alpha} \sum_{k_\alpha} T_{k_\alpha k'}^{\uparrow\uparrow} G_{k\uparrow k_\alpha\uparrow}^r(\varepsilon) + \sum_{\alpha} \sum_{k_\alpha} T_{k_\alpha k'}^{\uparrow\downarrow} G_{k\uparrow k_\alpha\downarrow}^r(\varepsilon) + \delta_{kk'}, \quad (12)$$

$$(\varepsilon - \varepsilon_{k'\uparrow} + M \cos \theta)G_{k\downarrow k'\uparrow}^r(\varepsilon) = -M \sin \theta G_{k\downarrow k'\downarrow}^r(\varepsilon) + \sum_{\alpha} \sum_{k_\alpha} T_{k_\alpha k'}^{\uparrow\uparrow} G_{k\downarrow k_\alpha\uparrow}^r(\varepsilon) + \sum_{\alpha} \sum_{k_\alpha} T_{k_\alpha k'}^{\uparrow\downarrow} G_{k\downarrow k_\alpha\downarrow}^r(\varepsilon), \quad (13)$$

$$(\varepsilon - \varepsilon_{k'\downarrow} - M \cos \theta)G_{k\uparrow k'\downarrow}^r(\varepsilon) = -M \sin \theta G_{k\uparrow k'\uparrow}^r(\varepsilon) + \sum_{\alpha} \sum_{k_\alpha} T_{k_\alpha k'}^{\downarrow\downarrow} G_{k\uparrow k_\alpha\downarrow}^r(\varepsilon) + \sum_{\alpha} \sum_{k_\alpha} T_{k_\alpha k'}^{\downarrow\uparrow} G_{k\uparrow k_\alpha\uparrow}^r(\varepsilon), \quad (14)$$

$$(\varepsilon - \varepsilon_{k'\downarrow} - M \cos \theta)G_{k\downarrow k'\downarrow}^r(\varepsilon) = -M \sin \theta G_{k\downarrow k'\uparrow}^r(\varepsilon) + \sum_{\alpha} \sum_{k_\alpha} T_{k_\alpha k'}^{\downarrow\downarrow} G_{k\downarrow k_\alpha\downarrow}^r(\varepsilon) + \sum_{\alpha} \sum_{k_\alpha} T_{k_\alpha k'}^{\downarrow\uparrow} G_{k\downarrow k_\alpha\uparrow}^r(\varepsilon) + \delta_{kk'}. \quad (15)$$

By combining Eqs. (8)–(15), we get a set of coupled equations

$$(\varepsilon - \varepsilon_{k'\uparrow} + M \cos \theta)G_{k\uparrow k'\uparrow}^r(\varepsilon) = -M \sin \theta G_{k\uparrow k'\downarrow}^r(\varepsilon) + \sum_{k''} A G_{k\uparrow k''\uparrow}^r(\varepsilon) + \sum_{k''} C G_{k\uparrow k''\downarrow}^r(\varepsilon) + \delta_{kk'}, \quad (16)$$

$$(\varepsilon - \varepsilon_{k'\uparrow} + M \cos \theta)G_{k\downarrow k'\uparrow}^r(\varepsilon) = -M \sin \theta G_{k\downarrow k'\downarrow}^r(\varepsilon) + \sum_{k''} A G_{k\downarrow k''\uparrow}^r(\varepsilon) + \sum_{k''} C G_{k\downarrow k''\downarrow}^r(\varepsilon), \quad (17)$$

$$(\varepsilon - \varepsilon_{k'\downarrow} - M \cos \theta)G_{k\uparrow k'\downarrow}^r(\varepsilon) = -M \sin \theta G_{k\uparrow k'\uparrow}^r(\varepsilon) + \sum_{k''} B G_{k\uparrow k''\downarrow}^r(\varepsilon) + \sum_{k''} C G_{k\uparrow k''\uparrow}^r(\varepsilon), \quad (18)$$

$$(\varepsilon - \varepsilon_{k'\downarrow} - M \cos \theta)G_{k\downarrow k'\downarrow}^r(\varepsilon) = -M \sin \theta G_{k\downarrow k'\uparrow}^r(\varepsilon) + \sum_{k''} B G_{k\downarrow k''\downarrow}^r(\varepsilon) + \sum_{k''} C G_{k\downarrow k''\uparrow}^r(\varepsilon) + \delta_{kk'}, \quad (19)$$

with

$$A = -\frac{i\Gamma_{L\uparrow}(\varepsilon)}{2} - \frac{i\Gamma_{R\uparrow}(\varepsilon)}{2} - \frac{i\gamma_2^2\Gamma_{L\downarrow}(\varepsilon)}{2} - \frac{i\gamma_4^2\Gamma_{R\downarrow}(\varepsilon)}{2},$$

$$B = -\frac{i\Gamma_{L\downarrow}(\varepsilon)}{2} - \frac{i\Gamma_{R\downarrow}(\varepsilon)}{2} - \frac{i\gamma_1^2\Gamma_{L\uparrow}(\varepsilon)}{2} - \frac{i\gamma_3^2\Gamma_{R\uparrow}(\varepsilon)}{2},$$

$$C = -\frac{i\gamma_1\Gamma_{L\downarrow}(\varepsilon)}{2} - \frac{i\gamma_3\Gamma_{R\uparrow}(\varepsilon)}{2} - \frac{i\gamma_2\Gamma_{L\uparrow}(\varepsilon)}{2} - \frac{i\gamma_4\Gamma_{R\downarrow}(\varepsilon)}{2},$$

where $\Gamma_{\alpha\sigma}(\varepsilon)$ is the linewidth function defined by $\Gamma_{\alpha\sigma}(\varepsilon) = 2\pi \sum_{k_\alpha} \rho(k_\alpha) |T_{k_\alpha\sigma k\sigma}|^2$ with $\rho(k_\alpha)$ as the density of states of electrons with momentum k_α and spin σ in the α FM electrode. For convenience, we introduce four parameters, $\gamma_1 = T_{k_L\downarrow}^\dagger/T_{k_L\uparrow}$, $\gamma_2 = T_{k_L\downarrow}^\dagger/T_{k_L\downarrow}$, $\gamma_3 = T_{k_R\downarrow}^\dagger/T_{k_R\uparrow}$, and $\gamma_4 = T_{k_R\downarrow}^\dagger/T_{k_R\downarrow}$, which characterize the spin-flip scattering effect. By considering the symmetry, we may further assume $\gamma_1 = \gamma_3$ and $\gamma_2 = \gamma_4$ for simplicity. The retarded Green's functions can be obtained in terms of Eqs. (16)–(19). On the other hand, the lesser self-energy can be approximated by Ng's ansatz:⁴⁰ $\Sigma^< = \Sigma_0^< (\Sigma_0^r - \Sigma_0^a)^{-1} (\Sigma^r - \Sigma^a)$, where $\Sigma^r - \Sigma^a = G^{r-1} - G^{a-1}$. Σ_0^r and $\Sigma_0^<$ are given by the following equations:

$$\begin{pmatrix} \Sigma_{0\uparrow\uparrow}^r & \Sigma_{0\downarrow\uparrow}^r \\ \Sigma_{0\uparrow\downarrow}^r & \Sigma_{0\downarrow\downarrow}^r \end{pmatrix} = \begin{pmatrix} -\frac{i\Gamma_{L\uparrow}(\varepsilon)}{2} - \frac{i\Gamma_{R\uparrow}(\varepsilon)}{2} & 0 \\ 0 & -\frac{i\Gamma_{L\downarrow}(\varepsilon)}{2} - \frac{i\Gamma_{R\downarrow}(\varepsilon)}{2} \end{pmatrix},$$

$$\begin{pmatrix} \Sigma_{0\uparrow\uparrow}^< & \Sigma_{0\downarrow\uparrow}^< \\ \Sigma_{0\uparrow\downarrow}^< & \Sigma_{0\downarrow\downarrow}^< \end{pmatrix} = \begin{pmatrix} i\Gamma_{L\uparrow}\left(\varepsilon + \frac{eV}{2}\right)f_L(\varepsilon) + i\Gamma_{R\uparrow}\left(\varepsilon - \frac{eV}{2}\right)f_R(\varepsilon) & 0 \\ 0 & i\Gamma_{L\downarrow}\left(\varepsilon + \frac{eV}{2}\right)f_L(\varepsilon) + i\Gamma_{R\downarrow}\left(\varepsilon - \frac{eV}{2}\right)f_R(\varepsilon) \end{pmatrix}.$$

After some algebras, we can arrive at

$$\tau^\theta = -\frac{1}{4\pi} \int d\varepsilon \text{Tr}_\sigma \left\{ (\sigma_1 \cos \theta - \sigma_3 \sin \theta) \Gamma_L \left(\varepsilon + \frac{eV}{2} \right) [f_R(\varepsilon) - f_L(\varepsilon)] G T_R \left(\varepsilon - \frac{eV}{2} \right) B G^a \right\}, \quad (20)$$

with

$$\Gamma_\alpha = \begin{pmatrix} \Gamma_{\alpha\uparrow} \\ \Gamma_{\alpha\downarrow} \end{pmatrix},$$

$B = (\Sigma_0^r - \Sigma_0^a)^{-1} (\Sigma^r - \Sigma^a)$, and $f_\alpha(\varepsilon)$ as the Fermi distribution function of the electrons in the α region. It is evident that these equations should be solved numerically in a self-consistent manner.

To proceed further the numerical calculations, we need to make some assumptions. Suppose that the two side FM electrodes are made of the same materials, i.e., $M_L = M_R$, $P_L = P_R = P$, where $P_{L(R)} = [\Gamma_{L(R)\uparrow} - \Gamma_{L(R)\downarrow}] / [\Gamma_{L(R)\uparrow} + \Gamma_{L(R)\downarrow}]$ is the polarization of the left (right) FM layer. Then, the linewidth function can be written as $\Gamma_{L\uparrow,\downarrow} = \Gamma_{R\uparrow,\downarrow} = \Gamma_0(1 \pm P)$, where $\Gamma_0 = \Gamma_{L(R)\uparrow}(P=0) = \Gamma_{L(R)\downarrow}(P=0)$ will be taken as an energy scale. $I_0 = \frac{e\Gamma_0}{\hbar}$ and $G_0 = \frac{e}{\hbar}$ will be taken as scales for the tunnel current and the differential conductance, respectively. The following material parameters are used for the middle FM: the uniaxial anisotropy field $H_k = 500$ Oe, the molecular field $M = 10\Gamma_0 \sim 1200$ Oe, where Γ_0 is taken as 20 meV, the Fermi level $130\Gamma_0$, $k_B T = 0.02\Gamma_0$, the damping coefficient $\alpha = 0.1$, and the junction area of 80×80 nm². The thickness of the middle FM is 5.6 nm throughout the paper unless it is specified otherwise.

III. SPIN-TRANSFER TORQUE

Let us first look at the case in absence of the spin-flip scatterings. The θ dependence of TMR, STT (τ^θ), as well as the ratio between the STT and electrical current (τ^θ/I) for different molecular fields (M) of the middle FM are presented in Figs. 2(a)–2(c). It is observed that the TMR increases strikingly with increase in the molecular field M at a given θ . The stronger the molecular field, the larger the TMR. The results also show that the STT as a function of θ behaves as a profile similar to a sine curve and vanishes when the relative alignment of magnetizations of the side FMs is parallel ($\theta=0$) or antiparallel ($\theta=\pi$) with respect to the middle FM. It is easily understood because the spin-

polarized electrons along the z or $-z$ axis cannot feel the spin-transfer effect owing to the property of $\hat{s}_{1,2} \times (\hat{s}_1 \times \hat{s}_2)$. However, the maximum values of the STT and their positions vary for different M . When θ is much less (larger) than $\pi/2$, the STT increases (decreases) with increasing the molecular field. From Fig. 2(c), one may find that τ^θ/I is also a nonmonotonic function of θ , and the maximum appears near $\theta = \pi/2$. It is interesting to note that τ^θ/I for different M has a crossing point at $\theta = \pi/2$.

The θ dependences of TMR, STT τ^θ , and τ^θ/I for different polarizations P of the side FMs are shown in Figs. 2(d)–2(f). It is no doubt that the larger the polarization P , the larger the TMR and the STT. This result suggests that the ferromagnetic materials with large polarization should be

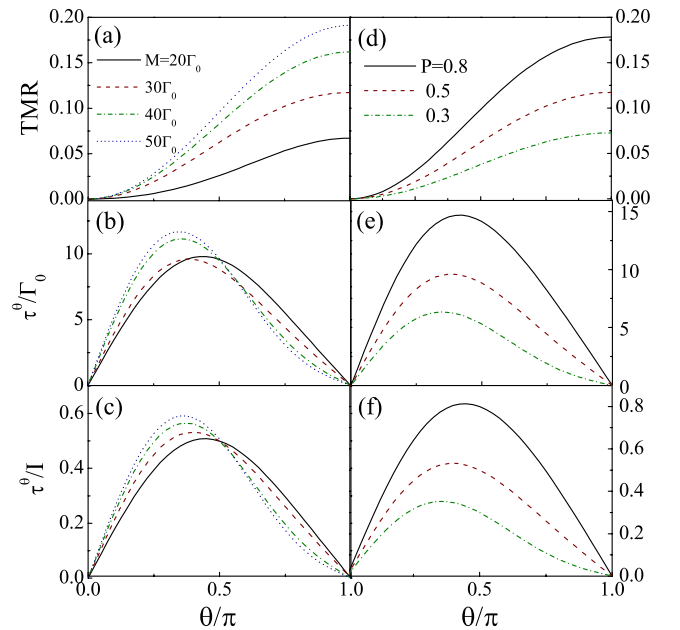


FIG. 2. (Color online) The angular dependence of (a) TMR, (b) spin-transfer torque τ^θ/Γ_0 , and (c) τ^θ/I for different M , where $P = 0.8$. The θ dependence of (d) TMR, (e) spin-transfer torque τ^θ/Γ_0 , and (f) τ^θ/I for different P , where $M = 30\Gamma_0$, $eV = 100\Gamma_0$.

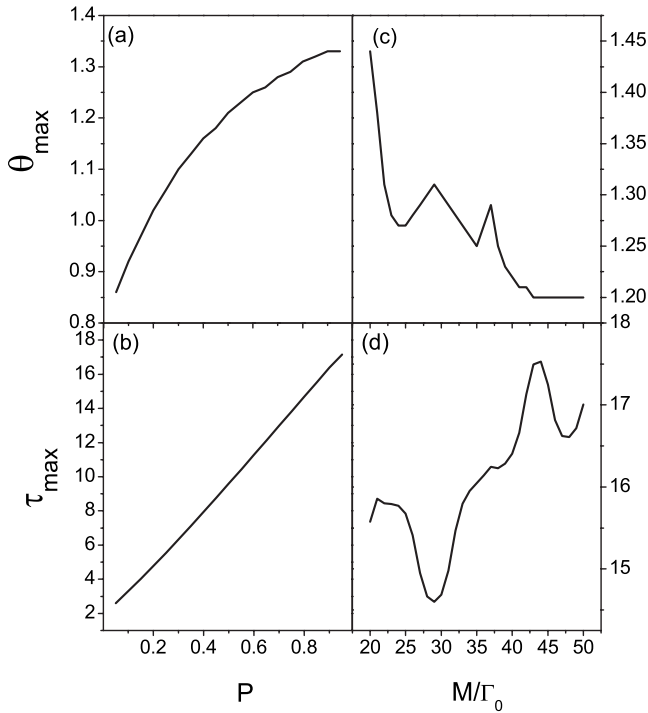


FIG. 3. The polarization dependence of (a) θ_{\max} and (b) τ_{\max}^{θ} and the molecular-field dependence of (c) θ_{\max} and (d) τ_{\max}^{θ} , where $eV = 100\Gamma_0$.

chosen if the STE as a mechanism is used to design a spintronic device, being consistent with the intuition.

At first glance, the property of the STT in the FM-FM-FM DBMTJ system is similar to the previous spin-valve systems. However, we will find the differences if we concentrate on the maximum of the STT τ_{\max}^{θ} and the corresponding angle θ_{\max} . In previous works, θ_{\max} decreases with increasing the polarization P while τ_{\max}^{θ} increases with increasing P .¹⁷ However, both maxima of the STT τ_{\max}^{θ} and θ_{\max} in the present system increase monotonically with P , as shown in Figs. 3(a) and 3(b). The M dependences of θ_{\max} and τ_{\max}^{θ} are also presented in Figs. 3(c) and 3(d). It is found that neither θ_{\max} nor τ_{\max}^{θ} is a monotonic function of M .

Now let us discuss the θ dependence of the tunnel current and the STT τ^{θ} in presence of the spin-flip scattering effect, as shown in Fig. 4. The angular dependence of the electrical current exhibits a cosinelike behavior, while the STT shows a sinelike behavior, a reminiscent of the spin-valve effect. It can be seen that the spin-flip effect leads to not only an imperfect spin-valve effect as the maximum of the tunnel current does not appear at $\theta=0$ but also a nonvanishing spin torque at $\theta=0$ or π . It appears that the spin-flip scatterings cause an additional spin torque in the parallel or antiparallel alignments of magnetizations between the middle and side FMs. This observation is similar to those uncovered in single-barrier MTJs.^{11,20} In addition, when $\gamma_1 = \gamma_2 = \gamma$, the angle shift is proportional to γ ; when $\gamma_1 \neq \gamma_2$, the effects of γ_1 and γ_2 on I/I_0 and τ^{θ}/Γ_0 are various. For instance, the behaviors for $\gamma_1=0.1, \gamma_2=0.2$ and $\gamma_1=0.2, \gamma_2=0.1$ look different, where the angle shift in the latter case is more obvious.

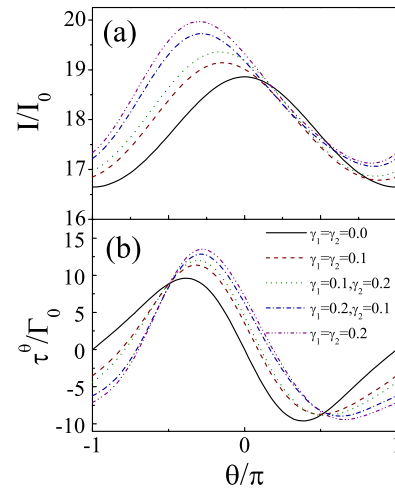


FIG. 4. (Color online) The angular dependence of (a) the tunnel current I and (b) the spin-transfer torque τ^{θ} for different γ_1 and γ_2 , where $P=0.8, M=30\Gamma_0$, and $eV=100\Gamma_0$.

The bias dependence of the current as well as the STT for different thicknesses L_m of the middle FM are shown in Fig. 5 when θ is nearly equal to zero (for instance, $\theta=0.005\pi$). We assume that the system can be viewed as a quantum well, and the lowest 20 energy levels of the middle region are included in the calculations. In Fig. 5, it is seen that the STT oscillates obviously with the bias for different thicknesses of the central FM. The oscillation varies for different L_m , while the electrical current is almost linear (but with slight oscillations) with increase in the bias. The oscillations origin from the quantum resonant tunneling of electrons, as the middle FM region is taken as a quantum well. When we change the thickness L_m of the middle FM, it gives rise to the shift of energy levels, leaving the resonant oscillations slightly different from various thicknesses but the qualitative behaviors look similar. As will be demonstrated later, it is this oscillating behavior of the STT with the bias that leads to unusual characteristics of the critical current for magnetization reversal.

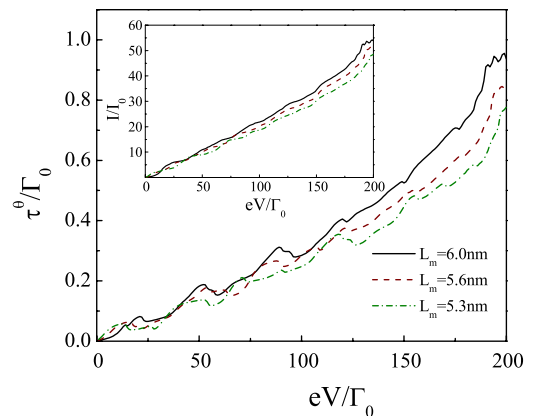


FIG. 5. (Color online) The bias dependence of the spin-transfer torque τ^{θ} and electrical current I (inset), where $M=15\Gamma_0$ and $P=0.7$.

IV. CRITICAL CURRENT FOR MAGNETIZATION REVERSAL

In terms of the STE, one can apply directly the electrical current to switch the magnetic state of a FM in absence of a magnetic field. It is this property of STE that makes it possible to fabricate the current-controlled spintronic devices, which is much expected in information industry, because using a current to manipulate a nanomagnetic device may be easier to realize in fabrication than using a magnetic field. Therefore, to enable to reverse the magnetization by a current through STE, there should exist a critical current at which the alignment of magnetic moments in a FM is reversed, which is more concerned in the device engineering. For this purpose, as the FM-FM-FM DBMTJ can be a basic element for MRAM and spin transistors, we shall pay attention to the critical current for magnetization reversal in the FM-FM-FM DBMTJ by invoking the Landau-Lifshitz-Gilbert (LLG) equation with inclusion of the STT. The generalized LLG equation can be written as⁴¹

$$(1/\gamma)\frac{d\hat{n}_m}{dt} = \hat{n}_m \times [\vec{H}_{\text{eff}} - \alpha\hat{n}_m \times (\vec{H}_{\text{eff}} + s\hat{n}_s)],$$

where γ is the gyromagnetic ratio $g\mu_B/\hbar$, α is the LLG damping coefficient, \hat{n}_s is a unit vector whose direction is that of the initial spin-polarized current, $\hat{n}_m = \vec{M}/|M|$, \vec{H}_{eff} is the effective magnetic field including the external field, the anisotropy field, the exchange field, the demagnetization field, and the random field, etc. The first two terms have been investigated extensively in the past decades, and the last term, the STT, is induced by the spin-polarized current which is under our interest.

According to Ref. 42, the critical field h_s , which is defined through $\vec{\tau} = s\hat{n}_m \times (\hat{n}_s \times \hat{n}_m) = 2l_m K h_s \hat{n}_m \times (\hat{n}_s \times \hat{n}_m)$ and deduced from the stability condition of the magnetization at $\theta=0$, reads

$$h_s = -\alpha \left(1 + h + \frac{1}{2}h_p \right), \quad (21)$$

where $K = \frac{1}{2}MH_k$, H_k is the Stoner-Wohlfarth switching field, $h = H/(2K/M)$, $h_p = K_p/K$, H is an applied field, and K_p is the easy-plane anisotropy energy that is assumed to be $2\pi M_s^2$ for a thin film.

In the previous work,⁴² the quantity s is assumed to be proportional to the electronic current: $s = (\hbar/2e)\eta I$, with $\eta = (I_\uparrow - I_\downarrow)/(I_\uparrow + I_\downarrow)$ as the spin-polarization factor of the incident current I , which can be treated as a constant. The critical current is given by

$$I_c = \frac{1}{\eta} \left(\frac{2e}{\hbar} \right) \alpha (a^2 l_m H_k M_s) \left(1 + \frac{2\pi M_s}{H_k} + \frac{H}{H_k} \right), \quad (22)$$

where M_s is the saturation magnetization and the magnetic field H is applied along the z axis. For a thin-film device with current-perpendicular geometry, we may assume that there are ways to neutralize the easy-plane anisotropy field, leading to the critical current $I_c = \frac{1}{\eta} \left(\frac{2e}{\hbar} \right) \alpha (a^2 l_m H_k M_s)$, which indicates that the current is proportional to M_s .

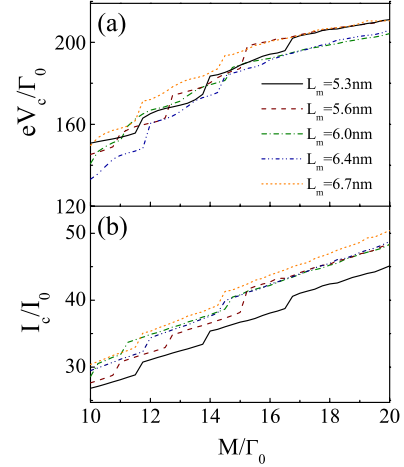


FIG. 6. (Color online) The molecular-field dependence of (a) critical voltage V_c and (b) critical current I_c for different L_m , where $P=0.7$.

However, our preceding calculations show that the relationship between STT and electrical current is more complicated than a simple proportionality. Therefore, it is not suitable to use Eq. (22) directly in our system, and a self-consistent way that incorporates the NEGF method and LLG equation should be adopted. For a given M , the critical field h_s and thus the critical spin torque τ_θ can be determined by Eq. (21) that was derived from the LLG equation. As τ_θ is a function of voltage and M , a proper voltage V should be chosen to get the critical τ_θ by the NEGF method. Once a critical voltage V_c is determined, the critical current is then obtained.⁴³

The relationship between the critical voltage, the critical current, and the molecular field M of the middle FM for different thicknesses L_m of the middle FM is presented in Fig. 6. It can be seen that it is much complicated than a linearity. The steps appear at different molecular fields for different L_m . The steplike behaviors of the critical voltage and current are not very unexpected. To switch the magnetic state of the middle FM, the larger the magnetization M , the larger the critical STT (τ_θ) is needed. However, the STT does not increase monotonously with the bias, which implies that in order to get the same amount of the STT, different biases are needed, and this causes steps in $M - eV_c(I_c)$ curves. Since the oscillations are various for different thicknesses of middle FM, the positions of steps appear at different places. Because of $I_0 = \frac{eI_0}{\hbar}$, the order of the critical current may be estimated from our calculations to be about $10^5 - 10^6$ A/cm², which is comparable to the results calculated for other systems.⁴²

Figure 7 shows the molecular-field dependence of the critical voltage and critical current for different polarizations P . We can see that with the increase in M , both V_c and I_c increase with steplike features. Not only the thickness of the middle FM but also the polarization P of the side FMs can influence the steplike characters of the critical voltage and current. The reason of the polarization P effecting on the steplike characters of the critical voltage and current is that the tunneling electrons with spin up and spin down have

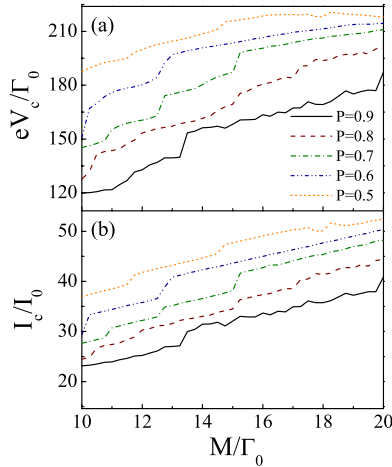


FIG. 7. (Color online) The molecular-field dependence of (a) critical voltage V_c and (b) critical current I_c for different P .

opposite spin-transfer effects on the middle FM. Because the electrons with different spins have different energy levels in quantum wells of the middle FM, the bias dependence of the STT induced by spin-up and spin-down electrons is different. When the polarization P is changed, the tunneling rate of spin-up and spin-down electrons is changed and so is the bias dependence of the total STT. As discussed above, the larger the polarization P , the larger the maximum of STT, which suggests that for larger P , even a small amount of tunneling electrons could generate the sufficient STT that enables to reverse the magnetization, leading to the observation that the larger P , the lesser the critical voltage (current) eV_c (I_c) is needed. By using the data of Fig. 7, we can depict the critical current versus the critical voltage, as shown in Fig. 8. It is observed that the relationship between I_c and V_c looks nearly linear in trend, and for different P , all curves of I_c against V_c almost fall into the same curve, in particular, at small V_c regions, which also reveals that the critical differential resistance remains almost constant with polarization P .

The relationships between the critical voltage, the critical current, and the polarization P of the side FMs for different M are also considered. The results are shown in Fig. 9. It is easy to see that the larger the polarization is, the smaller the critical voltage (current) is needed. However, the relationship between the critical voltage (current) and the polarization is

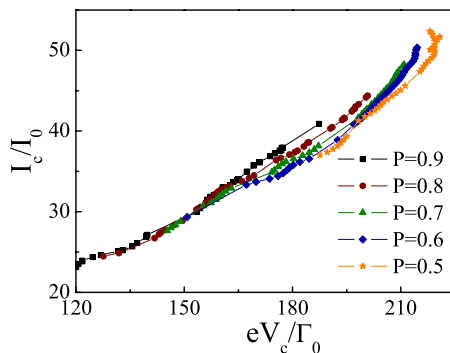


FIG. 8. (Color online) The critical current I_c versus critical voltage V_c for different P .

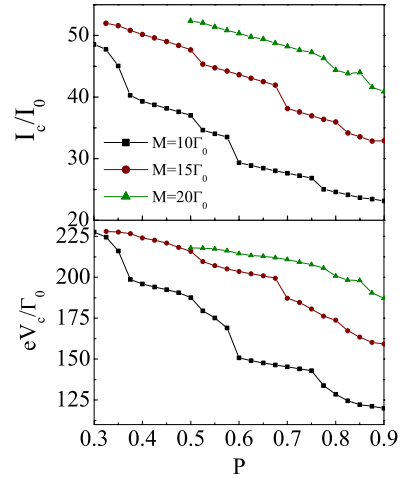


FIG. 9. (Color online) The polarization dependence of (a) critical voltage V_c and (b) the critical current I_c for different M .

not a simple linearity either; the steps are observed for different M that result from the resonant tunneling through quantum wells owing to the finite thickness of the middle FM. It is nontrivial to note that when the magnetization exceeds a certain value, some curves are ended. This is because the larger M , the larger critical STT is needed. However, for a smaller P , a smaller STT is obtained. So in some regions, the critical voltage and current cannot be procured by our self-consistent calculations.

V. SUMMARY

By means of the Keldysh nonequilibrium Green's-function method and invoking the generalized LLG equation with inclusion of the STT, we have systematically investigated the spin-transfer effect as well as the critical current for magnetization reversal in the FM-FM-FM DBMTJ system. The angular dependence of the TMR, the spin-transfer torques τ^θ and τ^θ/I for different molecular fields M of the middle FM, and the polarization P of the side FMs have been calculated. We have found that, in absence of spin-flip scatterings, the TMR increases dramatically with the increase in the molecular field of the middle FM, and the larger the molecular field, the greater the TMR. The angular dependence of the STT shows a shape similar to a sine curve. It is also observed that the larger the polarization of the side FMs, the greater the TMR and STT. In presence of the spin-flip scatterings, the angular dependence of the electrical current shows a cosinelike character, while the STT reveals a sine-like behavior. The spin-flip scatterings lead to an imperfect spin-valve effect. The STT is found to oscillate with the bias voltage for finite thickness of the middle FM, while the electrical current as a function of the bias is almost linear with slight oscillations. These oscillations may origin from the resonant tunneling from the quantum well states in the middle FM.

By applying the generalized LLG equation in presence of the STT, we have studied the critical current for magnetization reversal in the FM-FM-FM DBMTJ. It is uncovered that

the molecular-field dependence of the critical voltage and electrical current shows steplike behaviors for finite thicknesses of the middle FM. With increasing the molecular field of the middle FM, both the critical voltage and electrical current increase with steps. The order of magnitude of the critical current is estimated to be about 10^5-10^6 A/cm² in the system under interest, which is comparable with the previous results. The molecular-field dependence of the critical voltage and current shows a steplike increasing behavior with increasing M and, for a given molecular field of the middle FM, the larger the polarization P of the side FMs, the smaller the critical voltage and current. It has been unveiled that the relationship between V_c and I_c exhibits approximately a linear behavior, which is almost independent of polarization P of the side FMs. The polarization dependence of the critical current and voltage also shows a steplike decreasing behavior at a given M . These steplike behaviors of V_c and I_c are closely related to the fact that with increasing the bias voltage, the STT increases with oscillations, which

may be originated from the resonant tunneling between the quantum well states in the middle FM. Finally, we would like to remark that since the FM-FM-FM DBMTJ can be an important element for MRAM as well as spin transistors, our above-obtained results could provide useful information and guidance for choosing appropriate magnetic materials to fabricate the relevant spintronic devices.

ACKNOWLEDGMENTS

We are grateful to S. S. Gong, X. F. Han, W. Li, X. L. Sheng, Z. C. Wang, Z. Xu, Q. B. Yan, L. Z. Zhang, and G. Q. Zhong for helpful discussions. This work is supported in part by the National Science Fund for Distinguished Young Scholars of China (Grant No. 10625419), the National Science Foundation of China (Grants No. 90403036 and No. 20490210), the MOST of China (Grant No. 2006CB601102), and the Chinese Academy of Sciences.

*Author to whom correspondence should be addressed; gsu@gucas.ac.cn

¹M. N. Baibich, J. M. Broto, A. Fert, F. Nguyen Van Dau, F. Petroff, P. Eitenne, G. Creuzet, A. Friederich, and J. Chazelas, *Phys. Rev. Lett.* **61**, 2472 (1988).

²G. Binasch, P. Grünberg, F. Saurenbach, and W. Zinn, *Phys. Rev. B* **39**, 4828 (1989).

³M. Jullière, *Phys. Lett.* **54A**, 225 (1975).

⁴J. S. Moodera, L. R. Kinder, T. M. Wong, and R. Meservey, *Phys. Rev. Lett.* **74**, 3273 (1995); T. Miyazaki and N. Tezuka, *J. Magn. Magn. Mater.* **139**, L231 (1995).

⁵Y. M. Lee, J. Hayakawa, S. Ikeda, F. Matsukura, and H. Ohno, *Appl. Phys. Lett.* **90**, 212507 (2007).

⁶S. Mao, Y. Chen, F. Liu, X. Chen, B. Xu, P. Ru, M. Patwari, H. Xi, C. Chang, B. Miller, D. Menard, B. Pant, J. Loven, K. Duxstad, S. Li, Z. Zhang, A. Johnston, R. Lamberton, M. Gubbins, T. McLaughlin, J. Gadbois, J. Ding, B. Cross, S. Xue, and P. Ryan, *IEEE Trans. Magn.* **42**, 97 (2006).

⁷I. Žutić, J. Fabian, and S. D. Sarma, *Rev. Mod. Phys.* **76**, 323 (2004).

⁸Y. Tserkovnyak, A. Brataas, G. E. W. Bauer, and B. I. Halperin, *Rev. Mod. Phys.* **77**, 1375 (2005).

⁹G. Su, in *Progress in Ferromagnetism Research*, edited by V. N. Murray (Nova Science, New York, 2006), pp. 85–123.

¹⁰B. Jin, G. Su, Q. R. Zheng, and M. Suzuki, *Phys. Rev. B* **68**, 144504 (2003).

¹¹Z. G. Zhu, G. Su, Q. R. Zheng, and B. Jin, *Phys. Rev. B* **68**, 224413 (2003).

¹²Z. G. Zhu, G. Su, Q. R. Zheng, and B. Jin, *Phys. Rev. B* **70**, 174403 (2004).

¹³H. F. Mu, G. Su, Q. R. Zheng, and B. Jin, *Phys. Rev. B* **71**, 064412 (2005).

¹⁴B. Jin, G. Su, and Q. R. Zheng, *Phys. Rev. B* **71**, 144514 (2005).

¹⁵B. Jin, G. Su, and Q. R. Zheng, *Phys. Rev. B* **73**, 064518 (2006).

¹⁶L. Berger, *Phys. Rev. B* **54**, 9353 (1996).

¹⁷J. C. Slonczewski, *J. Magn. Magn. Mater.* **159**, L1 (1996).

¹⁸F. J. Albert, J. A. Katine, R. A. Burhman, and D. C. Ralph, *Appl. Phys. Lett.* **77**, 3809 (2000).

¹⁹M. Hosomi, H. Yamagishi, T. Yamamoto, K. Bessho, Y. Higo, K. Yamane, H. Yamada, M. Shoji, H. Hachino, C. Fukumoto, H. Nagao, and H. Kano, *Tech. Dig. - Int. Electron Devices Meet.* **2005**, 459.

²⁰Z. G. Zhu, G. Su, B. Jin, and Q. R. Zheng, *Phys. Lett. A* **306**, 249 (2003).

²¹H. F. Mu, Q. R. Zheng, B. Jin, and G. Su, *Phys. Lett. A* **336**, 66 (2005).

²²H. F. Mu, G. Su, and Q. R. Zheng, *Phys. Rev. B* **73**, 054414 (2006).

²³I. Theodonis, N. Kioussis, A. Kalitsov, M. Chshiev, and W. H. Butler, *Phys. Rev. Lett.* **97**, 237205 (2006).

²⁴Z. Z. Sun and X. R. Wang, *Phys. Rev. Lett.* **97**, 077205 (2006).

²⁵G. D. Fuchs, J. A. Katine, S. I. Kiselev, D. Mauri, K. S. Wooley, D. C. Ralph, and R. A. Burhman, *Phys. Rev. Lett.* **96**, 186603 (2006).

²⁶P. M. Levy and A. Fert, *Phys. Rev. Lett.* **97**, 097205 (2006).

²⁷J. A. Katine, F. J. Albert, R. A. Burhman, E. B. Myers, and D. C. Ralph, *Phys. Rev. Lett.* **84**, 3149 (2000).

²⁸Z. Li and S. Zhang, *Phys. Rev. Lett.* **92**, 207203 (2004).

²⁹K. Xia, P. J. Kelly, G. E. W. Bauer, A. Brataas, and I. Turek, *Phys. Rev. B* **65**, 220401(R) (2002).

³⁰G. D. Fuchs, I. N. Krivorotov, P. M. Braganca, N. C. Emley, A. G. F. Garcia, D. C. Ralph, and R. A. Burhman, *Appl. Phys. Lett.* **86**, 152509 (2005).

³¹S. Zhang, P. M. Levy, and A. Fert, *Phys. Rev. Lett.* **88**, 236601 (2002).

³²M. D. Stiles and A. Zangwill, *Phys. Rev. B* **66**, 014407 (2002).

³³T. Nozaki, N. Tezuka, and K. Inomata, *Phys. Rev. Lett.* **96**, 027208 (2006).

³⁴Y. Wang, Z. Y. Lu, X. G. Zhang, and X. F. Han, *Phys. Rev. Lett.* **97**, 087210 (2006).

³⁵Z. M. Zeng, X. F. Han, W. S. Zhan, Y. Wang, Z. Zhang, and S. F. Zhang, *Phys. Rev. B* **72**, 054419 (2005).

- ³⁶X. Chen, Q. R. Zheng, and G. Su, Phys. Rev. B **76**, 144409 (2007).
- ³⁷X. Waintal and P. W. Brouwer, Phys. Rev. B **63**, 220407(R) (2001).
- ³⁸X. Waintal and P. W. Brouwer, Phys. Rev. B **65**, 054407 (2002).
- ³⁹H. Haug and A. P. Jauho, *Quantum Kinetics in Transport and Optics of Semiconductors* (Springer, Berlin, 1998), p. 166.
- ⁴⁰T. K. Ng, Phys. Rev. Lett. **76**, 487 (1996).
- ⁴¹J. Z. Sun, IBM J. Res. Dev. **50**, 81 (2000).
- ⁴²J. Z. Sun, Phys. Rev. B **62**, 570 (2000).
- ⁴³Z. Li and S. Zhang, Phys. Rev. B **68**, 024404 (2003).